Progress In Electromagnetics Research C, Vol. 128, 219–229, 2023

Reactively Loaded Stripline Fed Rectangular Patch Antenna for Wireless and Biomedical Applications

Satheesh Rao*, Ashish Singh, Anil K. Bhat, Durgaprasad, and Krishnananda Shet

Abstract—In this article, two antennas having partial ground plane, slot loading with microstrip line feeding are proposed for wireless and biomedical applications. Antennas resonate at 2.4 GHz with two different bandwidths. The first antenna having 20% bandwidth, i.e., the Ultra Wide Band (UWB) of 2.10 GHz–2.61 GHz that can be utilized for wireless application and the Federal Communication Commission (FCC) allotted band of 2.36 to 2.39 GHz for medical applications falls in this range. The UWB antenna has undergone additional tuning to make it appropriate for biomedical application. Additionally a parametric analysis of antenna's slot length, width, and dielectric constant is performed to optimize the performance characteristics. The antenna is fabricated and tested using Vector Network Analyzer. The acquired results from simulation and measurement are in close match.

1. INTRODUCTION

These days the diagnosis of patients for acute diseases needs expensive and bulky equipment such as Magnetic Resonance Imaging (MRI), Computerized Tomography (CT) scan, and X-rays. These devices are capable of detecting various health issues such as tumors, malignant cells, fractures, stones, and foreign bodies. When patients are being scanned using such devices, patients are vulnerable to ionizing radiation. Moreover, scanning charges are high, and patients need to spend huge money for scanning. One of the leading causes of death is breast cancer. If being detected at an early stage of breast cancer the malignant cells can be cured completely thereby reducing the death rate related to breast cancer. A cost-effective method is necessary to undertake breast cancer screening tests at such an early stage. The microwave imaging using microstrip antenna (MSA) can be a good solution in this regard, and it also overcomes the major drawbacks of commercially available scanning devices.

An antenna is a sensing device that is effectively used in wireless communication [1–9]. Antenna can also be used for the scanning of patients' body after tuning to a prescribed Industrial, Scientific and Medical (ISM) band. UWB patch antennas are used in wireless communication and ISM bands [10]. The UWB antennas are used for transmitting or receiving short duration pulse. According to Federal Communication Commission (FCC), the antenna having bandwidth ≥ 500 MHz or bandwidth $\geq 20\%$ is classified as UWB antenna. In this view, UWB patch antenna [4] can be used for detecting health problems in the human body. UWB patch antenna can be used because of its small size and low fabrication cost. In literature different types of patch antennas have been reported for detecting breast cancer, tumor, and foreign body [10–17]. The different reported antennas for biomedical and wireless applications are UWB medical applications with on-body investigations, phase array, notch loaded, slot loaded, V-shape, proximity coupled, E-shaped, crescent shaped, etc. [2–17]. The above reported works have complicated geometry, missing theoretical analysis, or their bands do not lie in FCC [18] suggested band for body area network.

In this article, a patch antenna with strip line feeding and tuned defected ground plane has been proposed for the detection of tumor, breast cancer, fractures in muscles and bones. Antennas resonate at

Received 22 November 2022, Accepted 3 January 2023, Scheduled 16 January 2023
* Corresponding author: Satheesh Rao (satheesh.rao@nitte.edu.in).
The authors are with the E&C Department, NMAM Institute of Technology, Nitte, India.

2.4 GHz and 2.375 GHz with 500 MHz and 3 MHz bandwidths for wireless and biomedical applications, respectively.

2. ANTENNA GEOMETRY

The microstrip line fed patch antenna having rectangular ground plane is shown in Fig. 1. Antenna 1 has the radiating dimension of $(L \times W \times H)\,\text{cm}^3$ on which radiating patch has the dimension of $(L_{p1} \times W_{p1})\,\text{cm}^2$ with an inset fed microstrip line of dimension $(L_m \times W_{m1})\,\text{cm}^2$ excited via $50\,\Omega$ SubMiniature A (SMA) connector. Fig. 2 shows antenna 2 of a similar geometry to antenna 1 but differs in bandwidth and applications. Antenna 2 has a defected ground structure having a slot of dimension $(L_s \times W_s)\,\text{cm}^2$ with a patch of dimension $(L_{p1} \times W_{p1})\,\text{cm}^2$ with an inset fed microstrip line of dimension $(L_m \times W_m)\,\text{cm}^2$ and energized via a $50\,\Omega$ SMA connector. Both antennas are designed on an FR4 substrate having 1.6 mm of height with microstrip line feed. Table 1 shows the dimensions of designed antenna in cm. Fig. 3 shows fabricated antennas on an FR4 substrate.

Table 1. Dimensions of the Designed Antenna.

Parameter	Value (in cm)
L	5
W	5
W_{p1}	2
L_{p1}	3
W_p	2.210
L_p	2.45
W_{m1}	3
L_m	0.12
W_m	2.4
W_s	0.6
L_s	2.2
W_{s1}	1.345
H	0.16

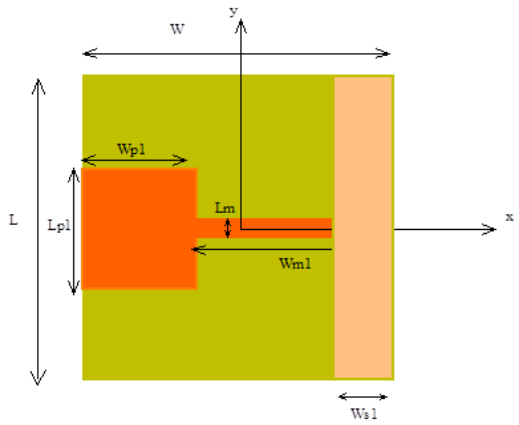

Figure 1. Proposed Antenna 1 for UWB Applications.

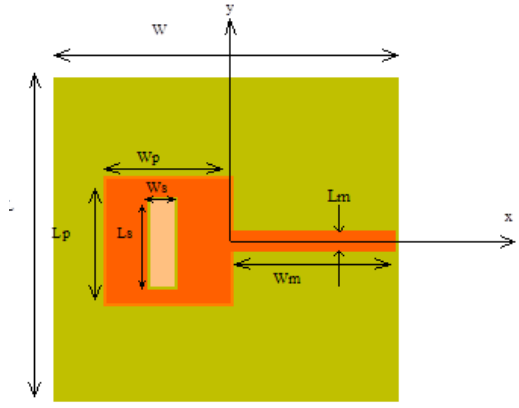

Figure 2. Proposed Antenna 2 for Biomedical Applications.

Figure 3. Fabricated Antenna Top and Bottom View.

2.1. Theoretical Analysis

The microstrip fed rectangular patch antenna can be represented by a high frequency radio frequency (RF) equivalent circuit shown in Fig. 4 as a combination of inductor, capacitor, and resistor and given as [19–21].

$$C_1 = \frac{LW\varepsilon_0\varepsilon_e}{2H}\cos^2\left(\frac{\pi X_0}{L}\right) \tag{1}$$

$$R_1 = \frac{Q}{\omega_r^2 C_1} \tag{2}$$

$$L_1 = \frac{1}{\omega_r^2 C_1} \tag{3}$$

L — length of inset fed patch; W — width of inset fed patch; H — thickness of antenna radiating area; ε_e — effective permittivity of substrate.

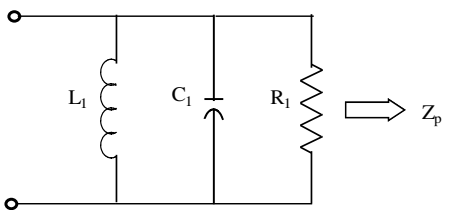

Figure 4. RF equivalent circuit for rectangular patch.

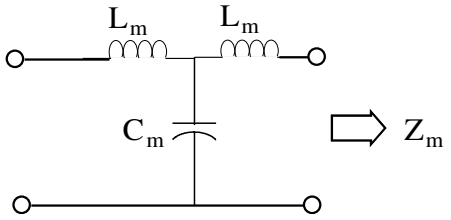

Figure 5. RF equivalent circuit for stripline.

The strip line of the high frequency radiating structure can be given as inductor L, capacitor C, and characteristic impedance Zo as shown in Fig. 5 and can be calculated as [19–23]

$$L_m = 100H\left(4\sqrt{\frac{W_s}{H}} - 4.21\right) \text{ nH} \tag{4}$$

$$C_m = W_s\{(9.5\varepsilon_r + 1.25)W_s/H + 5.2\varepsilon_r + 7.0\} \text{ pF} \tag{5}$$

The resonating frequency of the proposed antenna can be calculated

$$f = c/2L_e\sqrt{\varepsilon_{re}} \tag{6}$$

where

$$\varepsilon_{re} = 1/2[(\varepsilon_r + 1) + (\varepsilon_r - 1)(1 - 12H/W_s)^{-1/2} \tag{7}$$

Le = effective increase in the length of strip.

The input impedance Z_S of the slots is calculated as,

$$Z_S = R_S + jX_S \tag{8}$$

$$R_s = 60\left[C + \ln(kL_S) + \frac{1}{2}\sin(kL_S)\{S_i(kL_S) - 2S_i(kL_S)\} + 1/2\cos(kL_S) \left\{C - \frac{\ln(kL_S)}{2} - C_i(2kL_S) - 2C_i(kL_S)\right\}\right]\cos(\Psi) \tag{9}$$

$$X_s = 30[2S_i(kL_S) + \cos(kL_S)\{2S_i(kL_S) - S_i(2kL_S)\} - \sin(kL_S)\left\{2C_i(kL_S) - C_i(2kL_S) - C(2kW_S^2/L_S)\right\}] \tag{10}$$

Here C is the Euler's constant, Ψ the inclination of the slot from radiating edge, k the propagation constant, and functions $S_i(x)$ and $C_i(x)$ are defined as,

$$S_i(x) = \int_0^x \frac{\sin(x)}{x}dx \tag{11}$$

$$C_i(x) = -\int_0^\infty \frac{\cos(x)}{x}dx \tag{12}$$

where W_s is width of slots, and L_S is the Length of the slots. The equivalent circuit for slot is as in Fig. 6.

The coupling between upper microstrip patch and ground plane can be represented by another equivalent circuit as shown in Fig. 7.

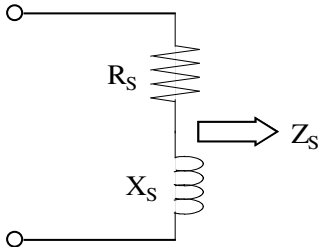

Figure 6. RF equivalent circuit for slot.

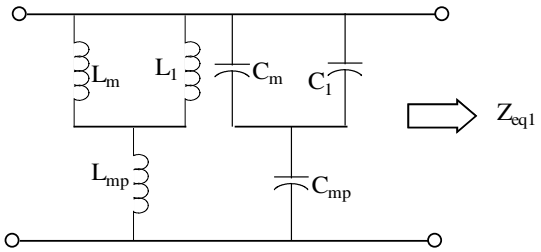

Figure 7. RF equivalent circuit for coupling between patch and ground.

L_{mp} and C_{mp} are mutual inductance and capacitance [24, 25] for the substrate, respectively.

$$L_{mp} = \frac{k_c^2(L_1 + L_m) + [k_c^4(L_1 + L_m)^2 + 4k_c^4(1 - k_c^2)L_1L_m]^{1/2}}{2(1 - k_c^2)} \tag{13}$$

$$C_{mp} = \frac{-(C_1 + C_m) + [(C_1 + C_m)^2 + (1 - 1/k_c^2)C_1C_m]^{1/2}}{2} \tag{14}$$

$$k_c = \frac{1}{\sqrt{Q_1Q_2}} \tag{15}$$

$$Q_1 = R_1\sqrt{\frac{C_1}{L_1}} \tag{16}$$

$$Q_2 = R_m\sqrt{\frac{C_m}{L_m}} \tag{17}$$

where Q_1 and Q_2 are the quality factor for two resonators, and R_m is the impedance of the microstrip.

L_{eq1} and C_{eq1} are the equivalent inductance and capacitance due to the electromagnetic coupling between top and bottom patches.

$$L_{eq1} = \frac{L_m L_1}{L_m + L_1} + L_{mp} \tag{18}$$

$$C_{eq1} = \frac{(C_m + C_1)C_{mp}}{C_m + C_1 + C_{mp}} \tag{19}$$

Hence the equivalent impedance Z_{eq1} is,

$$Z_{eq1} = \frac{1}{\left[\frac{1}{J\omega L_{eq1}} + J\omega C_{eq1}\right]} \tag{20}$$

The RF equivalent circuit of the proposed antenna is as shown in Fig. 8. Using this circuit model equivalent impedance Z_{in} can be computed. The resonant frequency is obtained from this network as

$$f_C = \frac{1}{2\pi\sqrt{LC}} \tag{21}$$

$$Z_{in} = Z_p||Z_m||Z_S||Z_{eq1} \tag{22}$$

The designed antenna is placed on the human body model. RF equivalent circuit for the complete simulation setup is as shown in Fig. 9. The body capacitance C_{body} depends on the dielectric characteristics of various tissues or organs of the human body, and R_{body} is the body resistance. As the dielectric properties of tumors vary from that of normal cells, C_{body} changes when tumors are present hence altering the resonant characteristics of the antenna.

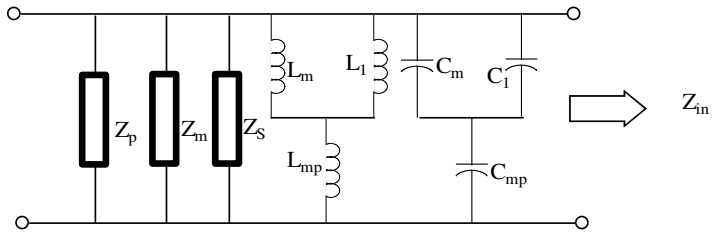

Figure 8. RF equivalent circuit for the proposed Antenna.

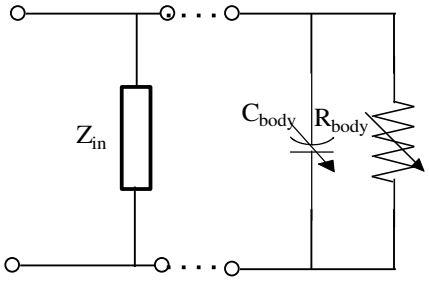

Figure 9. RF equivalent circuit for on body antenna placement.

3. RESULTS AND DISCUSSION

The designed antennas with partial ground and slot loaded ground are simulated, and the obtained results are shown in Fig. 10. It is observed that microstrip line with partial ground antenna has UWB at 2.4 GHz with band 2.09 GHz–2.62 GHz of 520 MHz having 21% bandwidth. Further, the same antenna has been tuned to specified medical band of 2.36 to 2.39 GHz using reactive loading at ground plane. Tumor and stone detection can be done using any antenna. However, reactive loaded antenna is more sensitive to detect tumors, etc. because of its narrow band, and the body reactance comes in parallel with this reactance making it more sensitive to change in body capacitance. Further this antenna band falls within FCC specified Medical Body Area Network (MBAN). Antenna with partial ground can be used for wide ranges for wireless application such as Bluetooth, ISM band 2.2–2.42 GHz, and MBAN band. Partial ground leads to wider bandwidth of the antenna making it suitable for these applications that require low power and higher data rate. Design and simulations are carried out in Computer simulation Technology (CST) Microwave Studio suite 2018.

The measured and simulated results with reflection coefficient and frequency are shown in Fig. 11. It is observed that simulated results are in good agreement with measured ones, and slight disagreement in

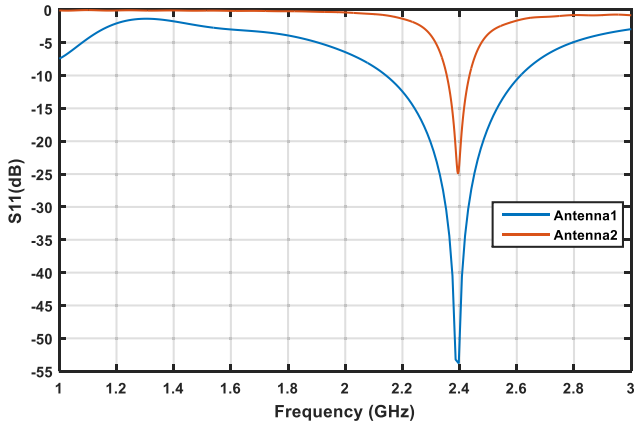

Figure 10. Reflection coefficient of Antenna 1 and Antenna 2.

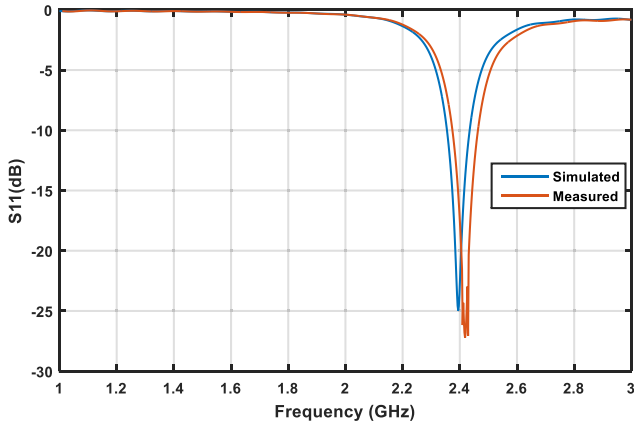

Figure 11. Measured and simulated results of inset fed slot loaded ground plane.

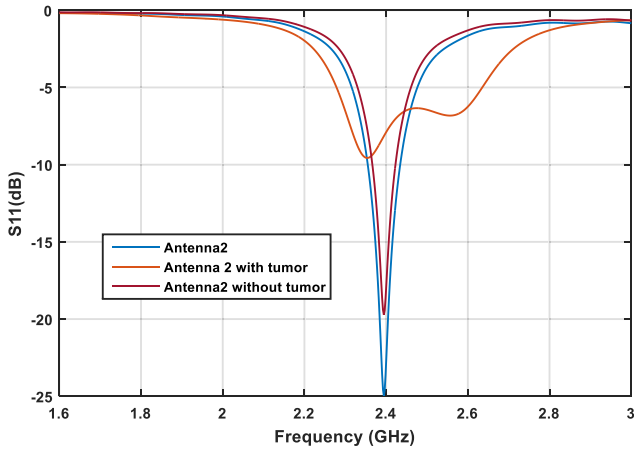

Figure 12. Simulated results of inset fed slot loaded ground plane with and without tumor.

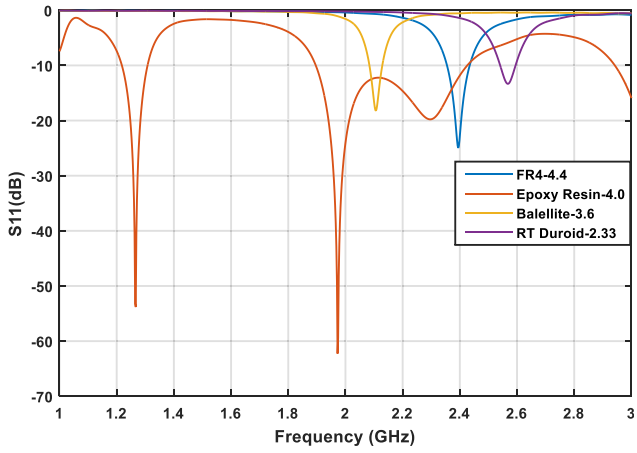

Figure 13. Variation of dielectric constant with frequency for inset fed slot loaded ground plane.

results is also visible due to uneven fabrication process of the antenna. Measured result shows resonating frequency at 2.44 GHz whereas simulated result shows resonating frequency at 2.39 GHz.

The antenna is placed on the human body model, and reflection coefficient is noticed for with and without tumor or deformities and is as shown in Fig. 12. It is observed that reflection coefficient without tumor is at -19 dB whereas that with tumor reflection coefficient moves up to -10 dB.

Fig. 13 shows the effect of varying dielectric constant on reflection coefficient against frequency. It is observed that with decreasing the dielectric constant from FR4 $\varepsilon = 4.4$ dielectric substrate to RT Duroid $\varepsilon = 2.33$, the resonating frequency shifts toward 3 GHz. It is also observed that multi-bands are observed at $\varepsilon = 4$ Epoxy Resin.

From Fig. 14 it is observed that increasing and decreasing the slot length L_s to 24 mm and 20 mm respectively leads to shifting of resonant frequency. With decreasing slot length resonance frequency shifts toward 2.6 GHz, and for $L_s = 24$ mm it shifts toward 2.18 GHz. This happens because of the change in reactance of the resonator. From Fig. 15 it is observed that with increasing slot width $W_s = 6$ mm to 8 mm resonance frequency moves to 2.5 GHz whereas with decreasing slot width $W_s = 6$ mm to 4 mm resonance frequency moves to 2.35 GHz. This occurs because of changing reactance of the antenna that changes resonating frequency of the antenna.

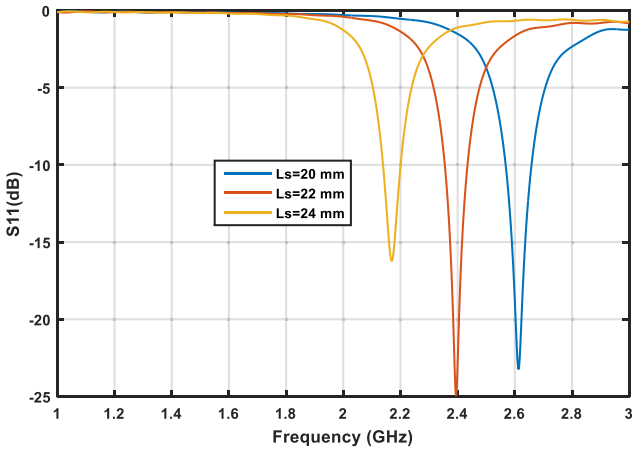

Figure 14. Variation of slot length L_s with frequency for inset fed slot loaded ground plane.

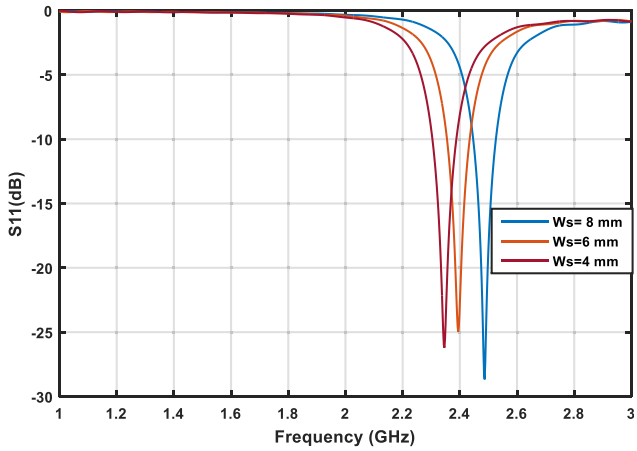

Figure 15. Variation of slot width W_s with frequency for inset fed slot loaded ground plane.

3.1. Specific Absorption Rate (SAR)

SAR term is used to define the radio frequency (RF) absorbed by human body when there is RF exposure on human body.

$$SAR\left(\frac{\mathrm{W}}{\mathrm{kg}}\right) = \frac{\sigma_m\left(\frac{\mathrm{S}}{\mathrm{m}}\right) \times E_m^2\left(\frac{\mathrm{V}}{\mathrm{m}}\right)}{M\left(\frac{\mathrm{kg}}{\mathrm{m}^2}\right)} \tag{23}$$

where E_m is the electric field (V/m), σ_m the conductivity of material (S/m), and M the mass density (kg/m^3).

The designed antenna is simulated on CST simulation software considering the following layer of body structure. The first antenna is placed at a distance of 1 mm from the body part, the skin of height 0.8–2.6 mm, fat of height 1.3–23.4 mm, muscle of height 0–30 mm, and bone of height 5.5–6.6 mm. These layers are visible in simulation as shown in Fig. 16. From Fig. 16 it is observed that with exposing antenna over body part at 2.4 GHz frequency, the noted SAR for 100 gm is 2.1181 W/kg. From the figure it is noticed that the maximum SAR is observed near the skin surrounding the antenna area whereas the remaining parts have minimum effect from 1 W/kg to 0.

To analyse the effect of antenna performance on human body CST Gustav Voxel model has been used, and antenna is placed just above the head, as shown in Fig. 17. Model was simulated on CST simulation tool. The maximum electric field, magnetic field, current density, electrical energy density, and power loss density of 10951.3 V/m, 41.492 A/m, 53.79 A/m^2, 203 µJ/m^3, and 9251.29 W/m^3 respectively were observed at 2.4 GHz.

3.2. Current Distribution

Figure 18 shows the current distribution of the antenna having partial ground. From Fig. 18 it is observed that unidirectional flow of current from microstrip line feed and maximum current of 265.5 A/m is observed at perimeter of the radiating antenna.

3.3. Radiation Pattern

Figure 19 shows the radiation patterns of partial ground antenna for E-plane and H-plane. Fig. 19(a) shows E-plane pattern at $\theta = 0°$, and antenna 3 dB beamwidth is 90°. Fig. 19(b) shows H-plane pattern at $\theta = 90°$, and observed beamwidth is 115.4°.

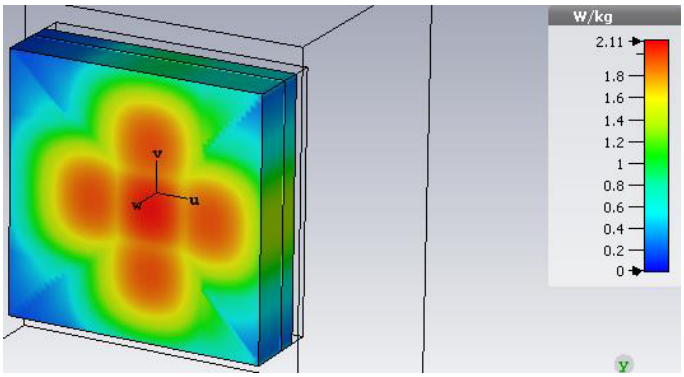

(a)

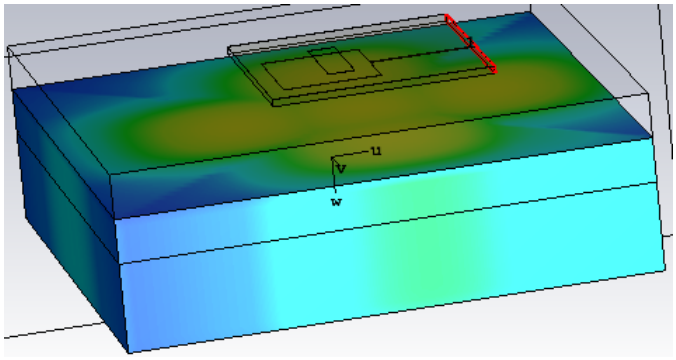

(b)

Figure 16. (a) SAR for reactive load ground antenna — top view. (b) SAR for reactive load ground antenna — side view.

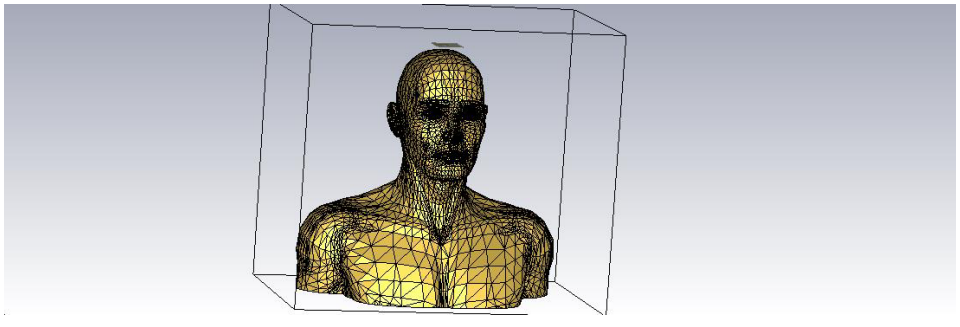

(a)

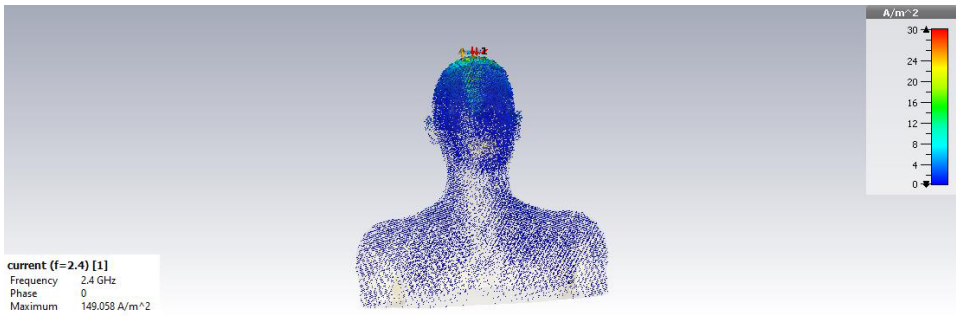

(b)

Figure 17. (a) Human model simulated on CST simulation tool [26]. (b) Human model simulated on CST simulation tool [26].

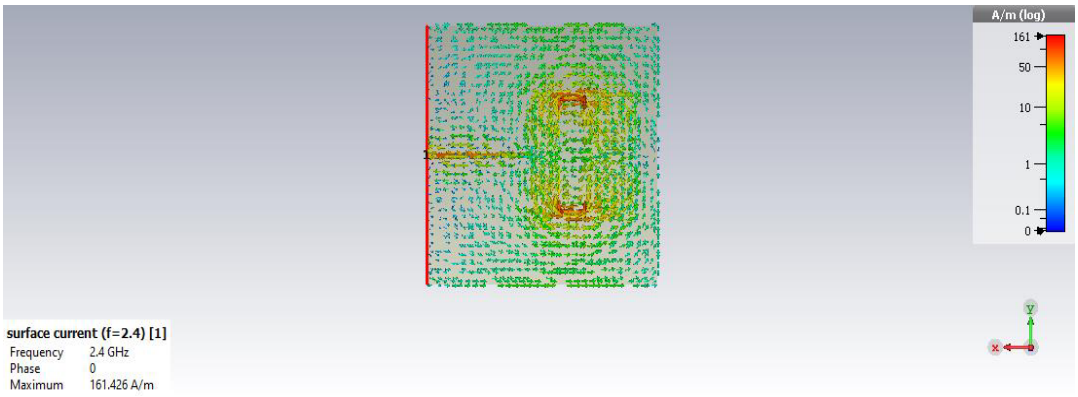

Figure 18. Current distribution of the partial ground antenna.

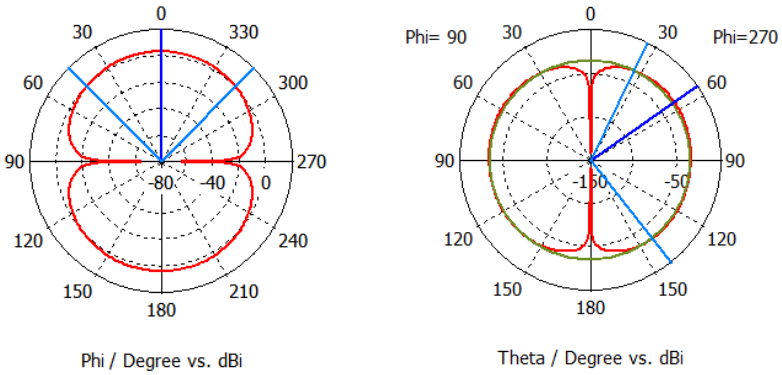

(a) (b)

Figure 19. (a) Radiation pattern of partial ground antenna for wireless application at 2.4 GHz — E Plane. (b) Radiation pattern of partial ground antenna for wireless application at 2.4 GHz — H Plane.

4. CONCLUSION

A microstrip line fed reactive loaded patch antenna for wireless and biomedical application has been designed, experimented and presented. The study also discusses the supporting RF equivalent circuit for the antenna and body model. Antenna characteristics observed at 2.4 GHz has shown excellent radiation pattern for wireless application such as Bluetooth, Industrial, Scientific and Medical (ISM) band 2.2–2.42 GHz, and Medical Body Area Network (MBAN) band. Meanwhile, the ground plane plays an important role in achieving 520 MHz and 3 MHz bandwidths. Reactive loading and partial ground concepts were used to make the antenna suitable for biomedical and UWB applications, respectively. The findings of the simulation show that antenna 2 can detect tumours with great clarity. Future work can be done on improving the bandwidth of the antenna.

REFERENCES

1. Chung, K. L. and C. H. Wong, "Wang-shaped patch antenna for wireless communication," *IEEE Antennas and Wireless Propagation Letters*, Vol. 9, 638–640, 2010.
2. Gosalia, K. and G. Lazzi, "Reduced size, dual-polarized microstrip patch antenna for wireless communications," *IEEE Transactions on Antenna and Propagation*, Vol. 51, 2182–2186, 2003.

3. Liang, Z., J. Liu, Y. Li, and Y. Long, "A dual-frequency broadband design of coupled-fed stacked microstrip monopolar patch antenna for WLAN applications," *IEEE Antennas and Wireless Propagation Letters*, Vol. 15, 1289–1292, 2016.
4. Elsadek, H. and D. M. Nashaat, "Multiband and UWB V-shaped antenna configuration for wireless communications applications," *IEEE Antennas and Wireless Propagation Letters*, Vol. 7, 89–91, 2008.
5. Li, P. K., Z. H. Shao, Q. Wang, and Y.J. Cheng, "Frequency-and pattern-reconfigurable for multistandard wireless applications," *IEEE Antennas and Wireless Propagation Letters*, Vol. 14, 333–336, 2015.
6. Minasian, A. A. and T. S. Bird, "Particle swarm optimization of microstrip antennas for wireless communication systems," *IEEE Transactions on Antennas and Propagation*, Vol. 61, 6214–6217, 2013.
7. Yang, F., X.-X Zhang, X. Ye, and Y. Rahmat-Samii, "Wide-band E-shape patch antennas for wireless communications," *IEEE Transactions on Antennas and Propagation*, Vol. 49. 1094–1100, 2001.
8. Bakariya, P. S., S. Dwari, M. Sarkar, and M. K. Mandal, "Proximity-coupled multiband microstrip antenna for wireless applications," *IEEE Antennas and Wireless Propagation Letters*, Vol. 14, 646–649, 2015.
9. See, C. H., R A. Abd-Alhameed, D. Zhou, T. H. Lee, and P. S. Excell, "A crescent-shaped multiband planar monopole antenna for mobile wireless applicatons," *IEEE Antennas and Wireless Propagation Letters*, Vol. 9, 152–155, 2010.
10. Tak, J., S. Woo, J. Kwon, and J. Choi, "Dual-band dual-mode patch antenna for on/off-body WBAN communications," *IEEE Transactions on Antennas and Wireless Propagation Letters*, Vol. 15, 348–351, 2016.
11. Kissi, C., et al., "Reflector-backed antenna for UWB medical applications with on-body investigations," *International Journal of Antennas and Propagation*, Vol. 2019, Article ID 6159176, 17 pages, 2019.
12. Nilavalan, R., I. J. Craddock, A. Preece, J. Leendertz, and R. Benjamin, "Wideband microstrip patch antenna design for breast cancer tumour detection," *IET Microwaves, Antennas & Propagation*, Vol. 1, 277–281, 2007.
13. Cheng, X., D. E. Senior, C. Kim, and Y.-K. Yoon, "A compact omni-directional self-packeged patch antenna with complementary split-ring resonator loading for wireless endoscope applications," *IEEE Transactions on Antennas and Wireless Propagation Letters*, Vol. 10, 1532–1535, 2011.
14. Conway, G. A. and W. G. Scanlon, "Antennas for over-body-surface communication at 2.45 GHz," *IEEE Transactions on Antennas and Propagation*, Vol. 57, 844–855, 2009.
15. Jofre, L., et al., "Medical imaging with microwave tomographic scanner," *IEEE Trans. on Biomedical Engg.*, Vol. 37, 303–311, 1990.
16. Deeksha, B., A. Sai Ravi Teja, E. Sai Laxshmi, M. Nikhil Eshwar, and A. Singh, "Electromagnetically coupled notches loaded patch antenna for bio-medical applications," *IEEE Conference IMPACT 2017*, 283–286, Aligarh University, 2017.
17. Bahl, I. J., S. S. Stuchly, and M. Stuchly, "A new microstrip radiator for medical applications," *IEEE Trans. on Microwave Theory and Techniques*, Vol. 28, No. 12, 1464–1469, Dec. 1980.
18. FCC, "Medical body area network measurement procedures," pub 670572D01MBANv01, 2015.
19. Bahal, I. J., *Lumped Elements for RF and Microwave Circuits*, Artech House, Boston, 2003.
20. Kumar, G. and K. P. Ray, *Broadband Microstrip Antenna*, Artech House, USA, 2003.
21. Bahal, I. J. and P. Bartia, *Microstrip Patch Antenna*, Artech House, 1980.
22. Singh, A., M. Aneesh, Kamakshi, and J. A. Ansari, "Analysis of microstrip line fed patch antenna for wireless communications," *Open Engineering*, Vol. 7, 279–286, 2017.
23. Singh, A., K. Shet, D. Prasad, A. K. Pandey, and M. Aneesh, "A review: Circuit theory of microstrip antennas for dual-multi- and ultra-widebands," *Modulation in Electronics and Telecommunications*, Intechopen, Book Chapter, 2020.

24. Balanis, C. A., *Antenaa Theory, Analysis and Design*, 2nd Edition, Wiley, New York, 1997.
25. Terman, F. E., *Electronic and Radio Engineer*, 15, Kagakasha, Tokyo, Japan, 1995.
26. *Computer Simulation Technology Microwave Studio Suite 2018*, 2018.